

Chapter 5

The Contact Dynamics Method

Katalin Bagi

Budapest University of Technology and Economics, Hungary

ABSTRACT

The Contact Dynamics method, developed still in the 1980s, was originally applied for granular assemblies because of its efficiency in simulating rapid granular flows or vibration problems of discrete systems. In the oldest models the elements were spherical and perfectly rigid, but later the application of polyhedral and deformable elements also became widespread, allowing for the reliable simulation of problems related to masonry structures. The basic unit of the analysis in Contact Dynamics is the pair of two randomly chosen elements. The essence of the method is to find the contact force vector between the two elements in such a way that during the analysed time step the elements should not overlap each other. At the considered time instant an iterative process sweeps along randomly chosen pairs over and over again, and gradually adjusts the estimated contact forces to get an improving approximation of a state that satisfies the dynamic equations of the system. The method is particularly advantageous for earthquake analysis of masonry structures.

INTRODUCTION

The NSCD (Non-Smooth Contact Dynamics) method was presented to the public at the end of the 1980ies by M. Jean and J.J. Moreau (Moreau, 1988; Jean & Moreau, 1992). Its first main field of application was granular mechanics: in comparison to previous discrete element techniques, the NSCD method turned out to be particularly fast and efficient when simulating granular flows, rapid avalanches, segregation, vibration problems of granular materials etc. Since the individual deformations of the grains are usually negligible in these problems, models consisting of perfectly rigid elements were mostly applied at that time. In the first versions the elements were mostly spherical, but later the application of polyhedral elements also became widespread. Contact Dynamics models brought significant scientific achievements in the field of the dynamics of granular materials. (While the original papers on NSCD were rather abstract and not very helpful in providing practice-oriented explanations how the method really worked, the paper of Unger and Kertész (2003) brought a leap forward: it gave a clear, detailed, code-writer-oriented introduction to the line of thought of the method, providing valuable help for those

DOI: 10.4018/978-1-5225-0231-9.ch005

who wanted to write their own code and also for those who just wanted to understand the main concept lying behind the software which they were applying in their researches.)

For masonry structures polygonal or polyhedral elements are obviously more suitable than spheres, and the deformability of the elements is often also important to take into consideration. Jean and Moreau (1992) and Jean (1999) introduced the basics of modelling masonry walls with deformable rectangular blocks in NSCD, and Jean developed the software called LMGC that gave realistic results for the quasi-static selfweight problem of a planar wall (Jean, 1999). Dubois extended the method, developed the open code LMGC90 (Dubois & Jean, 2006), and offered it to the research community not only for using it but also for further developments. LMGC90 can model rigid or deformable, 2D or 3D bodies of spherical or polyhedral shape. Since its release in the early 2000ies several scientists and engineers have applied it for different quasi-static or dynamic problems related to masonry mechanics.

Another available Contact Dynamics software is SOLFEC (Kozirara & Bićanić, 2008). SOLFEC aimed at providing a user friendly platform for testing formulations and solution methods. The code implements different (rigid, uniform-strain and finite element) block models, contact detection algorithms, and time integration techniques. SOLFEC is particularly powerful in modelling element deformability with the help of FEM subdivision. In order to have reasonable computation times for real problems, parallelization is also applied in SOLFEC.

The approach of the Contact Dynamics method is very different from other discrete element techniques often applied for masonry analysis, 3DEC (Cundall, 1988) or DDA (Shi, 1992) for instance. In NSCD the basic unit of the analysis is the pair of two randomly chosen elements (contacting or non-contacting). The essence of the method is to find the contact forces transmitted between the two elements of the pair in such a way that during the analyzed time step the two elements should not overlap each other. The contact force is set to zero if the elements would not touch each other without this contact force even at the end of the timestep, and a non-zero vector is chosen (satisfying conditions corresponding to the mechanical behavior of the contact) if the two elements have to be slowed down in order to avoid overlap. So the motion of the system is numerically simulated in time through finite time steps, but in such a way that at the considered time instant an iterative process sweeps along randomly chosen pairs of the system over and over again, and gradually adjusts the estimated contact forces to get an improving approximation of a state that satisfies the dynamic equations of the system.

Contact recognition and the determination of its geometrical data (i.e. point of action of the contact force, and the normal direction) for polyhedral shapes require more sophisticated techniques than the treatment of spherical elements. The “common plane concept”, a very efficient solution of the problem, is an advantageous and widely applied possibility, and it will be introduced in a forthcoming section.

Most discrete element methods represent the deformability of the elements either by using an internal FEM mesh in the elements (e.g. 3DEC), or by concentrating the deformations into the contacts, like in the case of PFC (Cundall & Strack, 1979). The calculation of the contact forces between the elements are based on the stiffness characteristics of the contacts in those techniques. The philosophy of NSCD is different. According to the oldest NSCD models, the elements are perfectly rigid, and the contact forces are not related to any stiffness data: the contact forces are calculated to ensure the dynamic equations of the elements, and in addition, they must not violate requirements like the Coulomb limit for friction or the no-tension requirement in cohesionless contacts, but their calculation does not apply any constitutive relations. For statically highly indeterminate systems like e.g. a masonry wall, there exist several alternative force systems that satisfy the equations of motion; NSCD produces randomly one of them, while several equally valid solutions can be received if the problem is calculated repeatedly with the method

The Contact Dynamics Method

starting from the same initial state, but considering the pairs of elements in different random orders. This non-uniqueness partly explains the doubts why NSCD is not widespread in the analysis of quasi-static problems. On the other hand, since the method is computationally very efficient for the simulation of dynamic problems, NSCD is more popular in earthquake simulations or vibration analysis. It has to be emphasized that there is a general lack of validation studies about the simulation of quasi-static as well as dynamic problems. The attempts of Ceh et al (2015a, 2015b) are very promising in this respect; similar verification examinations (static as well as dynamic) could potentially resolve the existing skepticism of the engineering community and give a fair general evaluation of the strengths and limitations of the technique. So this is a basically important task for future researches.

The aims of this chapter are (1) to provide an insight into how the method works; (2) to call the attention on the possible problems and questionable issues the user should be aware of; and (3) to present a collection of characteristic applications.

This Chapter is built up as follows. The basic concepts are presented in Section 2: for the sake of simplicity, in section 2 rigid elements are considered only. Section 3 focuses on deformable elements and calls the attention on the most important differences from the rigid-element model. Finally, Section 4 introduces different applications of the Contact Dynamics method in the analysis of masonry structures.

MODELLING WITH RIGID ELEMENTS

Geometrical Characteristics of the Pair of Two Elements

The Closest Points

Rigid elements in 3D have six degrees of freedom, 3 translational and 3 rotational. A reference point is defined on each element, usually coinciding with its centre of gravity (see Figure 1 for an illustration in 2D). Let us consider an arbitrarily selected pair of two elements not necessarily in contact with each other. State variables and the geometrical characteristics of this pair will be collected now.

Figure 1. Distance g^{pq} between elements p and q and the definition of vectors \mathbf{r}^{pc} and \mathbf{r}^{qc}

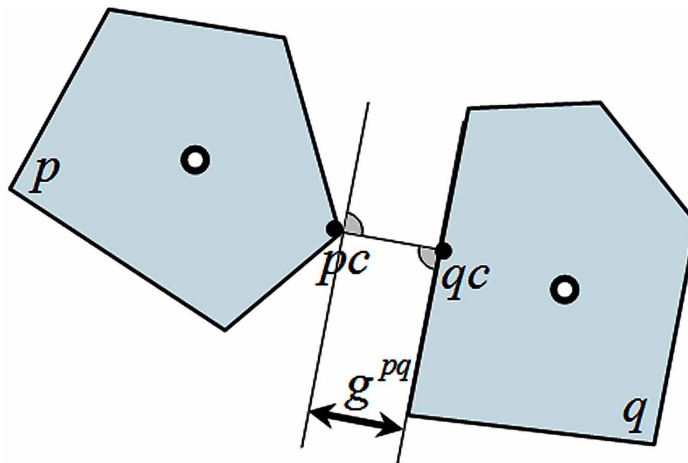


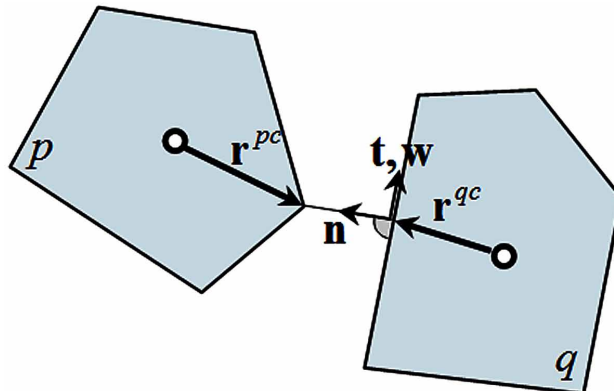
Figure 1 illustrates two elements, p and q . (Element p is the first and q is the second entity of the pair denoted by c .) In order to decide whether p and q are in contact at an actual time instant, the two nearest points on the boundary of p and q are determined (material points p_c and q_c respectively). In general they are node-to-face neighbours, as shown in Figure 1: in other words, assume for simplicity that the problem to find the two closest points has a unique solution. (The non-unique cases, i.e. edge-to-face neighbours when an edge lies in parallel to a face, or face-to-face neighbours when two planar faces lie parallel to each other, can be modelled as the simultaneous neighbouring pairs of a small finite number of node-to-face pairs).

Several possible algorithms are available to find the two closest points. The “common plane concept” is one of the most efficient techniques so this is applied in LMGC90 (Dubois & Mozul, 2013). This technique is also used in other discrete element codes, e.g. in 3DEC. The common plane can be imagined as a plate that is held loosely between the two polyhedral blocks. If the blocks are brought closer slowly, the plate will be moved by the blocks, and finally will become trapped at some particular position when the blocks come into contact. Whatever the shape and orientation of the blocks (provided they are convex), the plate will take up a position that defines the sliding plane for the two blocks. To carry the analogy a bit further, imagine that the plate is now repelled by the blocks even when they do not touch. As the blocks are brought together, the plate will take up a position midway between them, at a maximum distance from both. The algorithm for locating and moving the common plane can be formulated as an optimization problem: “Maximize the gap between the common plane and the closest vertex”. The optimization algorithm applies translations and rotations to the common plane in order to maximize the gap.

The normal vector of the common plane will serve as the contact normal, and the points having the shortest distances from the common plane are p_c and q_c . After finding the two closest points, sum up their distances from the common plane, and let g^{pq} denote this sum which is equal to the gap width between the two blocks.

Assign an $(\mathbf{n}, \mathbf{t}, \mathbf{w})$ local coordinate frame to the pair in the way shown in Figure 2. The unit base vector \mathbf{n} is directed towards the nearest point of p (first element of the pair). Base vectors \mathbf{t} and \mathbf{w} are an arbitrary pair of orthogonal unit vectors parallel to the contact plane. The g^{pq} distance is the \mathbf{n} -directional projection of the vector connecting the two closest points, oriented from q to p .

Figure 2. The local coordinate system of pair c



The Contact Dynamics Method

If this distance equals zero, the two elements form a point-like contact, and a concentrated contact force can be transmitted between the elements. Since the contact and the elements do not deform, the two elements must move in such a way that there would be no overlap between them: the gap width g^{pq} cannot become negative. In addition, the two elements can slide along each other (i.e. the two material points forming the contact point can translate relatively to each other in a direction perpendicular to \mathbf{n}) only if the frictional limit is reached in the contact.

The Reduced Contact Forces

When a contact exists, contact forces can be transmitted between material points pc and qc (they are at the same position in this case). These forces are the basic unknowns of the method; the essence of the NSCD technique is to determine them with an iterative solver (see Sections 2.3 and 2.4) at discrete time instants. The force exerted on p by q is \mathbf{f}^{pc} , and the force acting on q by p is \mathbf{f}^{qc} (note that $\mathbf{f}^{pc} = -\mathbf{f}^{qc}$):

$$\mathbf{f}^{pc} = \begin{bmatrix} F_x^{pc}(t) \\ F_y^{pc}(t) \\ F_z^{pc}(t) \end{bmatrix} \text{ and } \mathbf{f}^{qc} = \begin{bmatrix} -F_x^{pc}(t) \\ -F_y^{pc}(t) \\ -F_z^{pc}(t) \end{bmatrix},$$

They can be reduced to the reference points of p and q with the help of the $\mathbf{B}^{pc}(t)$ and $\mathbf{B}^{qc}(t)$ *transition matrices*, respectively:

$$\mathbf{B}^{pc}(t) = \begin{bmatrix} 1 & 0 & 0 \\ 0 & 1 & 0 \\ 0 & 0 & 1 \\ 0 & -r_z^{pc} & r_y^{pc} \\ r_z^{pc} & 0 & -r_x^{pc} \\ -r_y^{pc} & r_x^{pc} & 0 \end{bmatrix} ; \quad \mathbf{B}^{qc}(t) = \begin{bmatrix} 1 & 0 & 0 \\ 0 & 1 & 0 \\ 0 & 0 & 1 \\ 0 & -r_z^{qc} & r_y^{qc} \\ r_z^{qc} & 0 & -r_x^{qc} \\ -r_y^{qc} & r_x^{qc} & 0 \end{bmatrix}.$$

The vectors \mathbf{r}^{pc} and \mathbf{r}^{qc} point from the reference points to the contact. The reduced forces are then:

$$\mathbf{f}_{red}^{pc}(t) = \mathbf{B}^{pc}(t) \cdot \mathbf{f}^{pc}(t) \quad ; \quad \mathbf{f}_{red}^{qc}(t) = \mathbf{B}^{qc}(t) \cdot \mathbf{f}^{qc}(t).$$

Summarize these two forces into the 12-scalar *reduced contact force vector* of the pair:

$$\mathbf{f}^{pq}(t) = \begin{bmatrix} \mathbf{f}_{red}^{pc}(t) \\ \mathbf{f}_{red}^{qc}(t) \end{bmatrix}.$$

This vector will take part in the equations of motion of the pair.

The Relative Velocity

The vector \mathbf{v}^{pq} denotes the velocity vector of the (p, q) pair:

$$\mathbf{v}^{pq}(t) = \begin{bmatrix} \mathbf{v}^p(t) \\ \mathbf{v}^q(t) \end{bmatrix},$$

which can be expressed as the time derivatives of the displacements:

$$\mathbf{v}^p(t) = \begin{bmatrix} \frac{du_x^p(t)}{dt} \\ \frac{du_y^p(t)}{dt} \\ \frac{du_z^p(t)}{dt} \\ \frac{d\mathbb{E}_x^p(t)}{dt} \\ \frac{d\mathbb{E}_y^p(t)}{dt} \\ \frac{d\mathbb{E}_z^p(t)}{dt} \\ \frac{d\mathbb{E}_x^p(t)}{dt} \\ \frac{d\mathbb{E}_y^p(t)}{dt} \\ \frac{d\mathbb{E}_z^p(t)}{dt} \end{bmatrix} ; \quad \mathbf{v}^q(t) = \begin{bmatrix} \frac{du_x^q(t)}{dt} \\ \frac{du_y^q(t)}{dt} \\ \frac{du_z^q(t)}{dt} \\ \frac{d\mathbb{E}_x^q(t)}{dt} \\ \frac{d\mathbb{E}_y^q(t)}{dt} \\ \frac{d\mathbb{E}_z^q(t)}{dt} \\ \frac{d\mathbb{E}_x^q(t)}{dt} \\ \frac{d\mathbb{E}_y^q(t)}{dt} \\ \frac{d\mathbb{E}_z^q(t)}{dt} \end{bmatrix}.$$

Consider now those two material points, pc and qc , which form the contact. Their velocities, \mathbf{v}^{pc} és \mathbf{v}^{qc} , can be expressed again with the help of the $\mathbf{B}^{pc}(t)$ and $\mathbf{B}^{qc}(t)$ transition matrices:

$$\begin{aligned} \mathbf{v}^{pc}(t) &= \mathbf{B}^{pcT}(t) \cdot \mathbf{v}^p(t) \\ \mathbf{v}^{qc}(t) &= \mathbf{B}^{qcT}(t) \cdot \mathbf{v}^q(t) \end{aligned}.$$

The relative velocity of the contact is the difference of the velocities of the two material points pc and qc :

$$\mathbf{v}^{pq}(t) = \begin{bmatrix} \mathbf{v}_x^{pc}(t) \\ \mathbf{v}_y^{pc}(t) \\ \mathbf{v}_z^{pc}(t) \end{bmatrix} := \mathbf{v}^{pc}(t) - \mathbf{v}^{qc}(t)$$

which yields

$$\mathbf{v}^{pq}(t) = \mathbf{v}^{pc}(t) - \mathbf{v}^{qc}(t) = \left(\mathbf{B}^{pcT}(t) \cdot \mathbf{v}^p(t) \right) - \left(\mathbf{B}^{qcT}(t) \cdot \mathbf{v}^q(t) \right).$$

The Contact Dynamics Method

This vector shows the relative translational velocity of point pc with respect to point qc , so if the two points are already in contact, the \mathbf{n} -component of this vector must not be negative in order to avoid overlapping. The tangential component has to be zero if the contact is not sliding.

Mechanical Conditions

In Coulomb-frictional, no-tension contact models the following requirements are to be satisfied in every pair:

1. If the two elements touch each other, i.e. if $g^{pq} = 0$, then a contact force can be transmitted. If $g^{pq} > 0$, then there is no contact, and no contact force exist in the pair. The case $g^{pq} < 0$ is not possible.
2. The normal component of the contact force, N^{pq} , can only be negative, i.e. compressional, but otherwise its magnitude ($N^{pq} = \mathbf{f}^{pcT} \cdot (-\mathbf{n})$ or $N^{pq} = \mathbf{f}^{qcT} \cdot \mathbf{n}$) is arbitrary. The (N^{pq}, g^{pq}) relation is shown in Figure 3.

The magnitude of the tangential force \mathbf{T}^{pq} (having a t - and a w -directional component) is limited by the Coulomb friction law:

$$|\mathbf{T}^{pq}| \leq -\nu \cdot N^{pq}$$

where ν is the friction coefficient. Figure 4 illustrates this limitation: the vector of the tangential force must point from the origin either to inside the cone (non-sliding contact) or just to the surface of the cone (sliding contact).

As long as \mathbf{T}^{pq} is below the friction limit, the tangential component of the relative translation must be zero (elastic contact deformation is not possible). When reaching the friction limit, the contact starts to slide: the $\dot{g}^{pq}(t)$ relative velocity has to be just opposite to the direction of the \mathbf{T}^{pq} force (the tangential relative translation must not have a component perpendicularly to the frictional force reaching the limit), and the magnitude of \mathbf{T}^{pq} is equal to $-\nu \cdot N^{pq}$. The magnitude of the relative translation is not limited in the contact model, this can be determined from kinematical considerations.

Figure 3. Normal force vs. gap width in Contact Dynamics

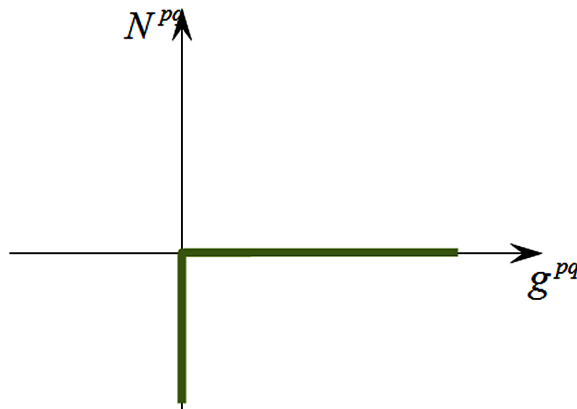
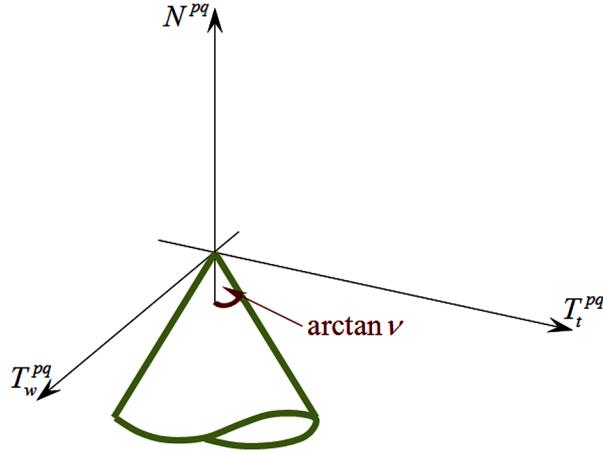


Figure 4. Coulomb limit for the tangential force



Without presenting the details, it is important to mention that Acary and Jean (2000) introduced more sophisticated and realistic representations of the real joint behaviour. They gave suggestions how to model finite tensional or shear resistance, elastic contact behaviour, brittle cohesion or progressive damage behaviour. These extensions of the joint modelling allow the user to give a realistic prediction for structures with mortared contacts. A wide range of such possibilities is available in LMGC90.

The Equations of Motion

Contact Dynamics is a time-stepping method: its fundamental unknowns are the time-dependent positions and velocities of the elements. They are searched for pair by pair.

Assume that at t_i the state of the system is known: according to the exactness numerically prescribed, the positions and velocities of the elements are given: $\mathbf{u}^p(t_i) \cong \mathbf{u}_i^p$; $\mathbf{v}^p(t_i) \cong \mathbf{v}_i^p$, and the external forces acting on the elements ($\mathbf{f}_i^{p,ext}$) and contact forces for all c (\mathbf{f}_i^{pc}) are also known. The external forces are reduced to the reference points; the contact forces act in the point-like contacts. The time-dependence of the external forces is also known (e.g. that the gravitational force is constant), so the external forces are given also in $t_{i+1} = t_i + \Delta t$ ($\mathbf{f}_{i+1}^{p,ext}$). From these data the state of the system at t_{i+1} (contact forces, the positions and the velocities of the elements) is searched for. Contact Dynamics applies the *implicit* version of the Euler method for this purpose. The basic step for the p and q pair can be written as:

$$\begin{bmatrix} \mathbf{v}_{i+1}^p \\ \mathbf{v}_{i+1}^q \end{bmatrix} := \begin{bmatrix} \mathbf{v}_i^p \\ \mathbf{v}_i^q \end{bmatrix} + \Delta t \cdot \begin{bmatrix} (\mathbf{M}^p)^{-1} \\ (\mathbf{M}^q)^{-1} \end{bmatrix} \cdot \begin{bmatrix} \mathbf{f}_{i+1}^p \\ \mathbf{f}_{i+1}^q \end{bmatrix};$$

$$\begin{bmatrix} \mathbf{u}_{i+1}^p \\ \mathbf{u}_{i+1}^q \end{bmatrix} := \begin{bmatrix} \mathbf{u}_i^p \\ \mathbf{u}_i^q \end{bmatrix} + \Delta t \cdot \begin{bmatrix} \mathbf{v}_{i+1}^p \\ \mathbf{v}_{i+1}^q \end{bmatrix}.$$

tions are already sufficiently close to the previous ones. When such a state is reached, the contact forces belonging to t_{i+1} have been found, and the next time step can follow.

The length of the timestep can be relatively large in comparison to models using explicit time integration (e.g. PFC or 3DEC). As explained by Radjai and Richefeu (2009), the limit on the timestep length is given by the occurrence of cumulative numerical errors leading to undesired excess overlaps between the particles. They suggest that a typical value for time step length is 10^{-4} sec for a system that consists of 10^4 rigid elements.

The approximation of the contact force in the pair (p, q) is based on the equations of motion of that pair. Before turning onto the details, a few notations have to be introduced:

For element p , reduce to the reference point all those forces (external and contact forces) acting at t_{i+1} , except from the force expressed by element q through contact c :

$$\mathbf{f}_{red,i+1}^{p,no-c} := \mathbf{f}_{i+1}^{p,ext} + \sum_{pk \neq pc} \mathbf{f}_{red,i+1}^{pk}.$$

The \mathbf{f}_{i+1}^{pk} contact force is only an actual approximation of the force indeed acting in contact pk at t_{i+1} ; it receives new and new values during the iterations. (At the beginning of the analysis of the time step the contact forces are approximated to be the same as their final, just determined values at the end of the previous time step, which is the same as the beginning of the just analysed timestep.)

Similarly, reduce all the forces acting at t_{i+1} on q – except from that force acting in qc – to the reference point of q :

$$\mathbf{f}_{red,i+1}^{q,no-c} := \mathbf{f}_{i+1}^{q,ext} + \sum_{qk \neq qc} \mathbf{f}_{red,i+1}^{qk},$$

and collect the two vectors into a hypervector:

$$\mathbf{f}_{red,i+1}^{pq,no-c} := \begin{bmatrix} \mathbf{f}_{red,i+1}^{p,no-c} \\ \mathbf{f}_{red,i+1}^{q,no-c} \end{bmatrix}.$$

Summarize the two transition matrices belonging to c into a hypermatrix:

$$\mathbf{B}^{pq} := \begin{bmatrix} \mathbf{B}^{pc} \\ -\mathbf{B}^{qc} \end{bmatrix}$$

and the matrices of inertia of p and q into a block-diagonal matrix, whose inverse is:

$$\left(\mathbf{M}^{pq}\right)^{-1} := \begin{bmatrix} \left(\mathbf{M}^p\right)^{-1} & \mathbf{0} \\ \mathbf{0} & \left(\mathbf{M}^q\right)^{-1} \end{bmatrix}.$$

The Contact Dynamics Method

Later the following two matrices will also be necessary:

$$\widetilde{\left(\mathbf{M}^{pq}\right)^{-1}} := \mathbf{B}^{pqT} \left(\mathbf{M}^{pq}\right)^{-1} \mathbf{B}^{pq},$$

and

$$\widetilde{\mathbf{M}^{pq}} := \left(\mathbf{B}^{pqT} \left(\mathbf{M}^{pq}\right)^{-1} \mathbf{B}^{pq} \right)^{-1}.$$

And now the equations of motion of the pair (p, q) can be compiled. First, the equations belonging to the end of the time interval can separately be written as:

$$\frac{1}{\Delta t} \begin{bmatrix} \mathbf{v}_{i+1}^p - \mathbf{v}_i^p \\ \mathbf{v}_{i+1}^q - \mathbf{v}_i^q \end{bmatrix} = \left(\mathbf{M}^{pq}\right)^{-1} \cdot \begin{bmatrix} \mathbf{f}_{red,i+1}^{p,no-c} + \mathbf{f}_{red,i+1}^{pc} \\ \mathbf{f}_{red,i+1}^{q,no-c} + \mathbf{f}_{red,i+1}^{qc} \end{bmatrix}.$$

Multiply both sides by \mathbf{B}^{pqT} from the left:

$$\begin{aligned} \frac{1}{\Delta t} \left[\mu_{i+1}^{pq} - \mu_i^{pq} \right] &= \mathbf{B}^{pqT} \left(\mathbf{M}^{pq}\right)^{-1} \cdot \mathbf{f}_{red,i+1}^{pq,no-c} + \\ &+ \mathbf{B}^{pqT} \left(\mathbf{M}^{pq}\right)^{-1} \mathbf{B}^{pq} \cdot \mathbf{f}_{i+1}^{pc} \end{aligned}$$

(it was taken into consideration that $\mathbf{f}_{i+1}^{qc} = -\mathbf{f}_{i+1}^{pc}$). After some rearrangements:

$$\mu_{i+1}^{pq} - \left(\mu_i^{pq} + \Delta t \cdot \mathbf{B}^{pqT} \left(\mathbf{M}^{pq}\right)^{-1} \cdot \mathbf{f}_{red,i+1}^{pq,no-c} \right) = \Delta t \cdot \widetilde{\left(\mathbf{M}^{pq}\right)^{-1}} \mathbf{f}_{i+1}^{pc}.$$

It is easy to notice that on the left side the vector in the parentheses means the relative velocity which would occur in the contact at t_{i+1} if \mathbf{f}_{i+1}^{pc} is zero, i.e. if there is no force in the contact. This vector will have a special importance in the forthcoming derivation, so a special notation is given to it:

$$\mu_{i+1}^{pq,no-c} := \left(\mu_i^{pq} + \Delta t \cdot \mathbf{B}^{pqT} \left(\mathbf{M}^{pq}\right)^{-1} \cdot \mathbf{f}_{red,i+1}^{pq,no-c} \right).$$

The equations of motion can now be written as:

$$\mu_{i+1}^{pq} = \mu_{i+1}^{pq,no-c} + \Delta t \cdot \widetilde{\left(\mathbf{M}^{pq}\right)^{-1}} \mathbf{f}_{i+1}^{pc}$$

where μ_{i+1}^{pq} and \mathbf{f}_{i+1}^{pc} are the unknowns. So the equations of motion give the relation between the unknown contact force and the unknown relative velocity belonging to the contact. This will be the starting point of the forthcoming calculations.

Finally the normal and tangential components of the relative velocity vector of the contact will be needed:

$$\mathfrak{v}_n^{pq} = \mathbf{n}^T \cdot \mu^{pq} ; \quad \mu_{tw}^{pq} = \mu^{pq} - \mathfrak{v}_n^{pq} \cdot \mathbf{n}$$

(Remember that μ^{pq} denoted the velocity of the material point pc relative to the material point qc . Hence a positive \mathfrak{v}_n^{pq} means increasing gap between the two material points.) Since the vector $\mu_{i+1}^{pq, no-c}$ belonging to the time instant t_{i+1} can directly be calculated from the already existing approximations of all other contact forces except from c , the components $\mathfrak{v}_{n, i+1}^{pq, no-c}$ and $\mu_{tw, i+1}^{pq, no-c}$ can also be determined, while the components of the vector μ_{i+1}^{pq} are unknowns.

The unknown μ_{i+1}^{pq} and \mathbf{f}_{i+1}^{pc} vectors are determined in three steps:

First decide whether the two elements will be in contact at t_{i+1} : calculate how large will the gap be between them, assuming zero contact force:

$$g_{i+1}^{pq, no-c} = g_i^{pq} + \mathfrak{v}_{n, i+1}^{pq, no-c} \cdot \Delta t .$$

A positive result means that there will be no contact at t_{i+1} , and the analysis of another pair can immediately follow. A negative result, on the other hand, means that without a contact force the elements p and q would overlap, so an \mathbf{f}^{pc} contact force is needed to avoid the overlap. In this case Step 2. follows.

Step 2: The contact force should modify the velocities of the two elements in such a way that instead of overlapping, they would exactly touch each other at the end of the time step. In Step 2. the aim is to determine \mathbf{f}_{i+1}^{pc} that satisfies the following two conditions:

- a. At t_{i+1} the gapwidth between p and q is exactly zero: $g_i^{pq} + \mathfrak{v}_{n, i+1}^{pq} \cdot \Delta t = 0$
- b. The contact does not slide, so the tangential component of the relative translation is zero:

$$\left| \mu_{tw, i+1}^{pq} \right| = 0$$

To satisfy these two conditions, the relative velocity of the contact should be:

$$\mu_{i+1}^{pq} = -\frac{1}{\Delta t} g_i^{pq} \cdot \mathbf{n}$$

(the negative sign means that if the gapwidth was larger than zero, then p should get closer to q to touch it).

The \mathbf{f}_{i+1}^{pc} has to be such a force that if continuously acting between p and q during (t_i, t_{i+1}) , at t_{i+1} the relative velocity would be just equal to \mathfrak{v}_{i+1}^{pq} . From the equations of motion, this force turns out to be equal to:

The Contact Dynamics Method

$$\mathbf{f}_{i+1}^{pc} = \frac{1}{\Delta t} \widetilde{\mathbf{M}}^{pq} \cdot \left(-\frac{1}{\Delta t} g_i^{pq} \mathbf{n} - \mu_{i+1}^{pq, no-c} \right).$$

Now the question is whether this force violates the constitutive conditions. There were two conditions on the components of the contact forces. The first one required the normal force a compression. This is automatically satisfied because of Step 1. The second one was the Coulomb-condition:

$$\left| \mathbf{T}_{i+1}^{pc} \right| \leq -\nu \cdot N_{i+1}^{pc}$$

If this holds for the calculated \mathbf{f}_{i+1}^{pc} , then the analysis of the (p, q) pair is ready, and a next pair can follow. However, if the tangential component exceeds the friction limit, then the calculated contact force cannot be transmitted in the contact: the contact slides, which means that the tangential component of μ_{i+1}^{pq} is not zero, and the calculation based on zero tangential component should be corrected. This correction is done in Step 3.

Step 3. In a sliding contact the tangential force component has to satisfy the following to conditions, and – as the third condition – the equations of motion:

- a. The contact is sliding, so the magnitude of the tangential force component is equal to the Coulomb-limit: $\left| \mathbf{T}_{i+1}^{pc} \right| = -\nu \cdot N_{i+1}^{pc}$
- b. The direction of the tangential relative velocity is just opposite to the direction of the tangential force component: $\frac{\mathbf{T}_{i+1}^{pc}}{\left| \mathbf{T}_{i+1}^{pc} \right|} = -\frac{\mu_{tw,i+1}^{pq}}{\left| \mu_{tw,i+1}^{pq} \right|}$

The equations of motion:

$$\mathbf{f}_{i+1}^{pc} = -\frac{1}{\Delta t} \widetilde{\mathbf{M}}^{pq} \cdot \left(\frac{1}{\Delta t} g_i^{pq} \mathbf{n} + \mu_{i+1}^{pq, no-c} - \mu_{tw,i+1}^{pq} \right)$$

From these conditions the unknowns \mathbf{f}_{i+1}^{pc} és μ_{i+1}^{pq} can be calculated, and the analysis of the (p, q) pair is ready. The next pair can follow.

These calculations introduced above give an approximation for the contact force in a pair, assuming that all other contact forces are unchanged and keep their values last approximated. When turning to the next pair, the latest approximations in other pairs are applied. Proceeding from pair to pair this way, an approximation is received for the whole system of contact forces. By sweeping through the complete set of contacts and nearly-contacting pairs over and over again, the results get closer and closer to what should exist at t_{i+1} . (Note that convergence is still an open issue: a precise proof does not exist in the literature.) The modifications caused by the consecutive iteration cycles cause smaller and smaller modifications in the contact forces; and the iteration can be terminated as the modifications decrease under a prescribed threshold. Now the state belonging to t_{i+1} has been found, and a new time step can be analysed.

The order according to which the pairs are considered within an iteration step is *random*; the only requirement is that every pair should be considered once within a step. In the next iteration step the starting pair and the ordering are different, prescribed also by a random number generator.

If the same problem is analysed twice, by starting the random number generator from two different initiations, the two resulting contact force systems will be different. This non-uniqueness of the solution has been emphasized by e.g. Jean (1999) or Moreau (2006). Indeed, for a statically highly indeterminate system several equilibrated force systems can be found, and without the flexibility data the “correct” one cannot be selected. In addition, the possibility of frictional sliding makes the solution history dependent. Moreau (2006) gave a very interesting discussion on the non-uniqueness of the solution. However, experiences on granular assemblies, e.g. Radjai and Richefeu (2009), show that though the order of the pairs greatly affect the individual contact forces and even the topology of the system, the overall, “macro” characteristics like average stress tensor or frequency diagram of contact force magnitudes remain the same, apart from slight statistical deviations. This conclusion might be valid for masonry systems too, but the existing investigations up to the present are still insufficient to draw reliable conclusions.

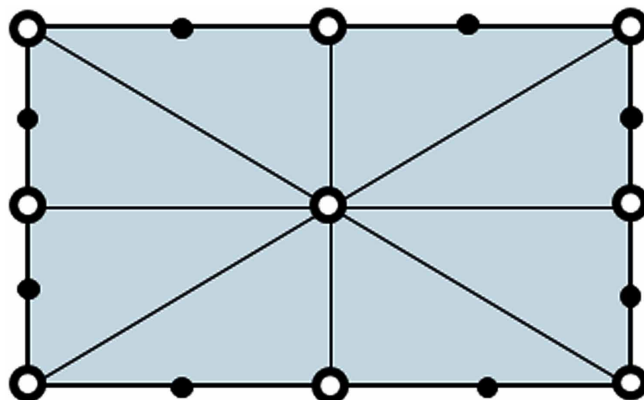
MODELLING WITH DEFORMABLE ELEMENTS

Elements and Contacts

Blocks in NSCD can be made deformable either by applying a uniform strain field in the whole block (like in DDA), or by using a finite element subdivision inside the blocks. Koziara and Bicanic (2008) presented the possibility to apply uniform-strain blocks. They used the term “pseudo-rigid bodies” to the approach, and suggested it as an intermediate model between perfectly rigid blocks and FEM-divided bodies. A finite element subdivision seems to be more appropriate for practical problems particularly in the case of complex block shapes or significantly varying stress fields inside the blocks.

Jean (1999) applied uniform-strain finite element subdivision as the simplest possibility for FEM meshing. A two-dimensional illustration is shown in Figure 5: a rectangular block is subdivided into eight uniform-strain triangular elements.

Figure 5. Deformable 2D block consisting of triangular finite elements: ○: nodes; ●: potential contact points



The Contact Dynamics Method

The mass of the element is distributed to the nodes (denoted by empty dots in Figure 5). The degrees of freedom are the translations of these nodes, which means that nodal rotations are not considered in the model: the usual strain field of classical continua is the basis of stress calculations (no Cosserat- or other non-classical continua are applied).

The equations of motion of a node specify the relations between the translational accelerations of the node, and between the forces reduced to the node:

- Mass-proportional forces (e.g. selfweight);
- External loads (including velocity-proportional forces like drag force);
- Contact forces acting on any face belonging to the analysed node;
- Internal forces: effect of stresses inside elements belonging to the analysed node.

The determination of the point where the contact forces act on the considered element is a crucial issue. Instead of performing a detailed analysis of the force distribution along the contact surfaces, a simplified approach is used. Dark dots in Figure 5 denote the candidates for contact points with neighbouring faces. They are chosen to be in the centre of the finite element face. Their actual position can be linearly interpolated from the nodes forming the face where the candidate contact point is located. If such a candidate touches a neighbouring face, contact forces act on the element at this contact point. The contact forces are then reduced to the nodes, according to the usual way at uniform-strain finite elements.

Note that LMGC90 offers more sophisticated FEM meshing options too (Dubois and Mozul, 2013), and in those cases the interpolation of contact point position and the reduction of the contact force become more complicated.

The Non-Uniqueness of the Solution

Similarly to the rigid-element case, the equations of motion of the whole system of deformable blocks at a time instant t can be written in the following general form:

$$\mathbf{M}\mathbf{a}(t) + \mathbf{C}\mathbf{v}(t) + \mathbf{K}(t)\Delta\mathbf{u}(t) = \mathbf{f}(t).$$

In this expression the meaning of the terms are as follows:

- $\Delta\mathbf{u}(t)$ is the hypervector containing the nodal translations from an initial deformation-free configuration to the actual nodal positions at t ;
- $\mathbf{v}(t)$ and $\mathbf{a}(t)$ are its first and second time derivatives (hypervectors of nodal velocities and nodal accelerations respectively);
- $\mathbf{K}(t)$ is the stiffness matrix expressing the elastic properties of the finite elements: its j -th column contains the opposite of nodal forces which arise when a unit translation is introduced at the j -th scalar of $\Delta\mathbf{u}(t)$;
- $\mathbf{C}(t)$ is the damping matrix: its j -th column contains the opposite nodal forces if a unit velocity occurs at the j -th scalar of $\mathbf{v}(t)$;

- $\mathbf{M}(t)$ is the block diagonal mass matrix that consists of as many blocks as the number of nodes, every block in it is a diagonal matrix containing three elements each of which being equal to the mass assigned to the corresponding node;
- $\mathbf{f}(t)$ is the hypervector of the external loads and contact forces reduced to the nodes.

Assuming that: (i) the structure is statically indeterminate or, at least, determinate, (ii) sliding, cracking or other abrupt changes of material behaviour can be excluded during $\Delta\mathbf{u}$, (iii) $\Delta\mathbf{u}$ is so small that \mathbf{K} remains approximately the same as in the initial configuration, and (iv) loads are quasi-static, then since the stiffness matrix is invertible and constant, the iterative solver introduced in Section 2.4 corresponds to a Gauss-Seidel relaxation solution of the equilibrium position corresponding to the given loads. In this case the solution would be unique. If the structure is kinematically indeterminate but nonlinearities do not occur, then \mathbf{K} is singular (though constant), and for general quasi-static loads the iterative solver does not lead to an equilibrium state but to an accelerating motion of the elements. (This phenomenon can characterize only an initial, small-displacement range of the behaviour.) Large displacements led to the gradual modification of \mathbf{K} . When sliding, contact cracking, or other dissipative material nonlinearities occur, \mathbf{K} varies, and the solution becomes history-dependent and non-unique. In this case (similarly to the rigid-element case) repeated solutions of the same problem may differ from each other. Even if the system converges to an equilibrium, there are various paths of motions possible, and they typically lead to different equilibrium states. The user should be aware of this feature of Contact Dynamics. Acary and Jean (2000) discuss the problem and suggest a few possibilities to deal with the issue.

APPLICATIONS

The Contact Dynamics Method has been rather popular among physicists studying granular dynamics problems (e.g. Daudon et al, 1997; Radjai et al, 1998; Unger et al, 2004). In the field of masonry mechanics most applications are related to seismic simulations, though a few examples on quasi-static analysis can also be found in the literature as shown by the applications below.

Chetouane et al (2005) applied the Contact Dynamics method for the simulation of Pont Julien, a 1st-century BC roman bridge in South France, in Vaucluse. They built a 2D model with dry frictional contacts, and compared the results provided by the rigid-element and the deformable-element modelling approaches for quasi-static case. The load was the selfweight of the structure. Principal stress directions, hydrostatic stress components and contact states were compared. They found that while the computation time was definitely longer, deformable elements provided more realistic results. The 3D analysis of the same bridge under the effect of flood was published in Rafiee and Vinches (2013). The selfweight of those parts of the structure being under water level was decreased according to buoyancy, and increasing crosswise horizontal forces acting on the pillars at different levels were tested. A variety of failure mechanisms were revealed.

Raiffee et al (2008a) modelled the Roman aqueduct in Arles, near Fontvielle, France. The aqueduct was collapsed, but the reasons of the failure were unknown. 3D rigid elements with dry frictional contacts were applied in the NSCD model of the aqueduct. Starting from an assumed undamaged initial geometry of the structure, selfweight and then sinusoidal seismic excitations were applied. The dynamic effects produced a cracked state of the structure, whose similarities to the in situ state suggested that a seismic event could be the reason of the destruction of the structure around 150 AD.

The Contact Dynamics Method

Rafiee et al (2008b) prepared 2D and 3D models of the amphitheatre in Nimes, one of the most beautiful and best preserved Roman arenas. The elements were rigid and deformable in their 2D models, and rigid in the 3D model, with dry contacts in all cases. In addition to selfweight, an artificial seismic vibration was simulated. The most vulnerable parts of the structure could be identified this way, so that a future restoration can take this knowledge into consideration. The amphitheatre was analysed a few years later by Bagn eris et al (2013), also with LMGC90. Rigid 3D elements were applied to model a similar part of the arena as in Rafiee et al (2008b). In Bagn eris et al (2013) the results provided by the rigid-element model were then applied to an individual block at the bottom of a pillar, and the behaviour of this block was simulated by using deformable elements in a linearly elastic FEM model. The pressure acting on this block along its boundaries was made non-uniform in the FEM analysis, in different ways (a peripheral support and surface roughness was produced by randomly translating the position of the FEM nodes perpendicularly to the surface). The results show that at some locations the magnitude of principle stresses could increase with 1 or even 2 orders of magnitude because of the contact surfaces being not perfectly planar. This phenomenon may lead to local damages that may modify the distribution of the internal forces in the structure provided by the NSCD calculation. (The authors also considered the effect of water infiltration, but that analysis is already out of the scope of an introduction to the NSCD method.)

Isfeld and Shrive (2015) modelled the cross-section of the wall of Prince of Wales Fort (built in the early 18th century) in Canada. The external part of the wall is made of cut stones lying on each other on approximately planar faces, while the core of the wall consists of rubble-like uncut stone pieces. The old mortar between the stone blocks degraded, weakened and was washed out during the centuries. In the model the external stones were represented by rigid polygons and the core consisted of rigid circular elements. The contacts were cohesive: the normal and shear strength were set to several different values in the different tests, and for every case the walls were tried to be equilibrated under selfweight. It was decided this way whether for the different joint material parameters the walls were stable or unstable. (The typical failure modes were also determined.) The authors concluded that stability could be improved by injecting grout into the walls.

Lancioni et al (2013) analysed a medieval Italian church, Santa Maria in Portuno. After its enlargement in the 11th century, the building had a nave and two aisles. For today only the nave remained, and one of the aims of the numerical analysis was to verify whether the collapse of the aisles could be caused by a 13th-century earthquake in the region. The authors applied rigid 3D polyhedral elements with dry frictional contacts. The geometry of the structure was reconstructed from the ruins that were found on the site. The model consisted of four macro-elements, corresponding to the following four main components of the structure: (1) the faade, (2) a longitudinal wall of the nave, (3) and external wall, and (4) the three apses. The 2009 L'Aquila earthquake was simulated. The analysis pointed out the most dangerous collapse mechanisms, and conclusions could be drawn regarding the expedient reinforcement of the structure.

Though the above examples demonstrate that the Contact Dynamics technique is able to simulate practical problems in an apparently realistic way, most of the applications up to now are poor in (or completely lack) a quantitative validation of the applied numerical model. An industry-inspired attempt to improve this situation can be found in the recent publications Ceh et al (2015a, 2015b). The authors conducted laboratory experiments and SOLFEC simulations on the same problem: multiple-block stacks subjected to base accelerations were analysed in both ways. Well-documented experimental and numerical tests like this would be very valuable for engineers who plan to apply a Contact Dynamics software for practical problems. With more validation studies, and with sufficiently increasing hardware capacities

in the forthcoming years, the Contact Dynamics method may become a powerful tool in the everyday engineering practice in masonry analysis.

ACKNOWLEDGMENT

The above study was supported by the Hungarian National Research Fund under grant no. OTKA 100770.

REFERENCES

- Acary, V., & Jean, M. (1998). Numerical simulation of monuments by the contact dynamics method. In *Procs. Monument-98 Workshop on seismic performance of monuments*.
- Acary, V., & Jean, M. (2000). Numerical modeling of three-dimensional divided structures by the Non Smooth Contact Dynamics method: Application to masonry buildings In *Procs. Fifth International Conference on Computational Structures Technology*.
- Bagneris, M., Dubois, F., & Martin, A. (2013). Numerical analysis of historical masonry structures for stone degradation diagnosis: An application to the Roman Amphitheater of Nîmes. In *2013 Digital Heritage International Congress (DigitalHeritage)*. doi:10.1109/DigitalHeritage.2013.6743792
- Camenen, J.-F., Ceh, N., Jelenic, G., Koziara, T., & Bicanic, N. (2015). Dynamic Sensitivity of a Multi-block Stack Subjected to Horizontal Harmonic Excitation. *22ème Congrès Français de Mécanique*, Lyon, France.
- Ceh, N., Pellegrino, A., Camenen, J.-F., Bicanic, N., Petrinic, N., & Tuhtan, M. (2015b). *Overturing of multiple-block stack - dynamic sensitivity parameters and scaling effect*. 8th International Congress of Croatian Society of Mechanics, Opatija, Croatia.
- Ceh, N., Pellegrino, A., Camenen, J.-F., Petrinic, N., Jelenic, G., Koziara, T., & Bicanic, N. (2015a). Dynamic sensitivity of multi-block stacks subjected to pulse base excitation – Experimental evidence and non-smooth contact dynamics simulations. In *Procs. COMPDYN 2015*.
- Chetouane, B., Dubois, F., Vinches, M., & Bohatier, C. (2005). NSCD discrete element method for modelling masonry structures. *International Journal for Numerical Methods in Engineering*, 64(1), 65–94. doi:10.1002/nme.1358
- Cundall, P. A. (1988). Formulation of a three-dimensional distinct element model - Part I: A scheme to detect and represent contacts in a system composed of many polyhedral blocks. *International Journal of Rock Mechanics and Mining Sciences*, 25(3), 107–116. doi:10.1016/0148-9062(88)92293-0
- Cundall, P. A., & Strack, O. D. L. (1979). A discrete numerical model for granular assemblies. *Geotechnique*, 29(1), 47–65. doi:10.1680/geot.1979.29.1.47
- Daudon, D., Lanier, J., & Jean, M. (1997). A micromechanical comparison between experimental results and numerical simulation of a biaxial test on 2D granular material. In Behringer et al. (Eds.), *Powders and Grains 97* (pp. 219–222). Balkema.

The Contact Dynamics Method

Dubois, F., & Jean, M. (2006). The non smooth contact dynamic method: recent LMGC90 software developments and application. In P. Wriggers & U. Nackenhorst (Eds.), *Analysis and Simulation of Contact Problems* (Vol. 27, pp. 375–378). Lecture Notes in Applied and Computational Mechanics. doi:10.1007/3-540-31761-9_44

Dubois, F., & Mozul, R. (2013). LMGC90. In *CSMA 2013, 11e Colloque National en Calcul des Structures*.

Isfeld, A., & Shrive, N. (2015). Discrete Element Modeling of Stone Masonry Walls With Varying Core Conditions: Prince of Wales Fort Case Study. *International Journal of Architectural Heritage*, 9(5), 564–580. doi:10.1080/15583058.2013.819135

Jean, M. (1999). The non-smooth contact dynamics method. *Computer Methods in Applied Mechanics and Engineering*, 177(3-4), 235–257. doi:10.1016/S0045-7825(98)00383-1

Jean, M., & Moreau, J. J. (1992). Unilaterality and dry friction in the dynamics of rigid body collections. In *Procs. Contact Mechanics International Symposium*. Presses Polytechniques et Universitaires Romandes.

Koziara, T. & Bićanić, N. (2008). Semismooth Newton method for frictional contact between pseudo-rigid bodies. *Computer Methods in Applied Mechanics and Engineering*, 197(33-40), 2763–2777.

Lancioni, G., Lenci, S., Piattoni, Q., & Quagliarini, E. (2013). Dynamics and failure mechanisms of ancient masonry churches. *Engineering Structures*, 56, 1527–1546. doi:10.1016/j.engstruct.2013.07.027

Moreau, J. J. (1988). Unilateral contact and dry friction in finite freedom dynamics. In J. J. Moreau & P. D. Panagiotopoulos (Eds.), *CISM Courses and Lectures* (Vol. 302). Vienna: Springer. doi:10.1007/978-3-7091-2624-0_1

Moreau, J. J. (2006). Facing the plurality of solutions in nonsmooth mechanics. In C.C. Baniotopoulos (Ed.), *Nonsmooth/Nonconvex Mechanics with Applications in Engineering, II. NNMAE 2006 (Proc. International Conference in Memoriam of P. D. Panagiotopoulos)*.

Radjai, F., & Richefeu, V. (2009). Contact dynamics as a nonsmooth discrete element method. *Mechanics of Materials*, 41(6), 715–728. doi:10.1016/j.mechmat.2009.01.028

Radjai, F., Wolf, D. E., Jean, M., & Moreau, J. J. (1998). Bimodal character of stress transmission in granular packings. *Physical Review Letters*, 80(1), 61–64. doi:10.1103/PhysRevLett.80.61

Rafiee, A., & Vinches, M. (2013). Mechanical behaviour of a stone masonry bridge assessed using an implicit discrete element method. *Engineering Structures*, 48, 739–749. doi:10.1016/j.engstruct.2012.11.035

Rafiee, A., Vinches, M., & Bohatier, C. (2008a). Application of the NSCD method to analyse the dynamic behaviour of stone arched structures. *International Journal of Solids and Structures*, 45(25-26), 6269–6283. doi:10.1016/j.ijsolstr.2008.07.034

Rafiee, A., Vinches, M., & Bohatier, C. (2008b). Modelling and analysis of the Nimes arena and the Arles aqueduct subjected to a seismic loading, using the Non-Smooth Contact Dynamics method. *Engineering Structures*, 30(12), 3457–3467. doi:10.1016/j.engstruct.2008.05.018

Shi, G.-H. (1992). Discontinuous deformation analysis: A new numerical model for the statics and dynamics of deformable block structures. *Engineering Computations*, 9(4), 157–168. doi:10.1108/eb023855

Unger, T., & Kertész, J. (2003). The contact dynamics method for granular media. In *Modeling of Complex Systems* (pp. 116–138). Melville, NY: American Institute of Physics. doi:10.1063/1.1571300

Unger, T., Wolf, D. E., & Kertész, J. (2004). *Force indeterminacy in the jammed state of hard disks*. cond-mat/0403089

KEY TERMS AND DEFINITIONS

Common Plane: The plane between two arbitrarily-shaped convex bodies which maximizes the gap between the plane and the closest points on the two elements.

Implicit Method: A time integration method is implicit if the approximated numerical solution of the differential equation of the analyzed initial value problem is calculated at the end of a time interval from the numerical solution at the beginning of the interval in such a way that the differential equation is satisfied at the end of the time interval according to any required exactness.

Iterative Solver: That part of an NSCD code which iteratively finds the approximate solution for contact forces at a given time instant.

Singular Stiffness Matrix: Structures that are not supported sufficiently, either internally or externally, are kinematically indeterminate. The stiffness matrix of such a structure is singular i.e. it has at least one zero eigenvalue, so that it cannot be inverted.

Time Integration: A procedure to quantitatively approximate the solution of an initial value problem described by a differential equation. The time integration provides quantitative approximations of the state variables of the modelled system at a series of separate time instants.